Preparation of grafting copolymer of acrylic acid onto loess surface and its adsorption behavior

Fengqin Tang, Di Gao, Li Wang, Yufeng He, Pengfei Song and Rongmin Wang

ABSTRACT

Loess is a typical natural mineral particle distributed widely around the world, and it is inexpensive, readily accessible, and harmless to the environment. In this study, loess was modified by surface grafting copolymerization of functional monomers, such as acrylic acid, N-vinyl pyrrolidone, and N,N-methylenebisacrylamide as a cross-linking agent, which afforded a novel loess-based grafting copolymer (LC-PAVP). After being characterized by scanning electron microscopy, thermal gravimetric analysis and Fourier-transform infrared spectroscopy, its adsorption capacity and mechanism of removing lead ions (Pb^{2+}) were investigated. With the study of the optimal experimental conditions, it was demonstrated that the removal rate of Pb^{2+} by LC-PAVP can reach up to 99.49% in 60 min at room temperature. It was also found that the kinetic characteristics of the adsorption capacity due to the pseudo-second-order kinetic model and the thermodynamics conformed well with the Freundlich model. In summary, as a lost-cost and eco-friendly loess-based adsorbent, LC-PAVP is a good potential material for wastewater treatment.

Key words | adsorption of lead ions, loess, surface modification, wastewater treatment

Fengqin Tang
Di Gao
Li Wang
Yufeng He
Pengfei Song
Rongmin Wang (corresponding author)
Key Laboratory of Eco-functional Polymer Materials of the Ministry of Education, Institute of Polymer, College of Chemistry and Chemical Engineering,
Northwest Normal University,
Lanzhou 730070,
China
E-mail: *wangrm@nwnu.edu.cn*

HIGHLIGHTS

- The silane coupling agents, a typical active functional groups, were introduced to the surface of loess particles.
- The copolymer of acrylic acid and N-vinyl pyrrolidone was coupled to the surface of loess particles by grafting polymerization.
- Loess is a cheap and easily available green silicate mineral.
- The loess grafting copolymer (LC-PAVP) showed excellent activity as a new adsorption material in wastewater treatment.
- The amount of polymer is reduced, and the production cost of polymer adsorbent is significantly lowered.

GRAPHICAL ABSTRACT

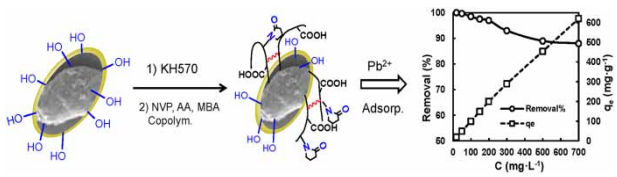

INTRODUCTION

Among all the heavy metals, lead ions (Pb^{2+}) are one of the most common and abundantly available pollutants in the environment (Arfin & Tarannum 2019). Pb^{2+} is nonbiodegradable and easily accumulated in living organisms for a

doi: 10.2166/wst.2020.359

long time (Zhang *et al.* 2011; Hashemzadeh *et al.* 2019), causing threatening diseases. In general, most of the current heavy metal removal technologies, including chemical precipitation (Fu *et al.* 2012), ion-exchange (Lasheen *et al.* 2016), reverse osmosis, and electrochemical and membrane process (Song *et al.* 2011) are costly and inefficient for pollutants (Liu *et al.* 2018). Hence, the effective and economic removal of heavy metals from wastewater is exceedingly important. In the past decades, adsorption technology was considered as the most efficient and inexpensive method compared to the other methods described above.

Various kinds of competent adsorbents have been reported, such as biosorbents (Shen *et al.* 2009) and activated carbon (Gong *et al.* 2007), maize husk adsorbent (Indah *et al.* 2016) and clay minerals like montmorillonite (Kumar *et al.* 2012; Yang *et al.* 2020), bentonite (Ecer *et al.* 2018), and apatite (Li *et al.* 2019) etc. Loess soil is widely distributed throughout Asia, Russia, the Middle East, and North America, and is especially abundant in China, covering an area of approximate 640,000 km^2 (Wang *et al.* 2009). As a wastewater treatment material, loess is an inexpensive and easily obtained eco-friendly silicate mineral that has been modified by many existing methods to improve its adsorption performance. However, in a previous study, the polymers were physically composited with loess (He *et al.* 2012; Shen *et al.* 2019), and therefore, the disadvantages were that the proportion of loess in composite is too low and its cost is high.

In this study, a novel surface grafted functional copolymer (LC-PAVP) was synthesized by grafting copolymerization, which produced to a remarkable adsorbent that was used to remove Pb^{2+} from aqueous solution. During preparation, the proportion of clay in the composite material was increased and the amount of polymer was reduced, and thus the production cost of polymer adsorbent was significantly decreased. As a new absorbent material, LC-PAVP was used in wastewater treatment. The optimal conditions to remove Pb^{2+} and adsorption mechanism of LC-PAVP were also investigated.

EXPERIMENTAL SECTION

Materials and reagents

Loess clay (LC) was collected in Lanzhou, China. After being ground, it was sieved with a 100 mesh, and then stored in a desiccator for further use. Hydrochloric acid (AR, HCl) was supplied by Beijing Chemical Plant. γ-Methacryloxypropyl trimethoxysilane (AR, KH-570) was supplied by Shanghai Jingchun Reagent Co. Ltd. Acrylic acid (AR, AA) was provided by Tianjin BASF Chemical Co. Ltd. N-vinyl pyrrolidone (AR, NVP) was provided by Xuzhou Zhuoyuan Chemical Co. Ltd. *N,N*-methylenebisacrylamide (AR, MBA) was purchased from Shanghai Zhongqin Chemical Reagent Co. Ltd. Acetic acid (AR, CH_3COOH) was supplied by Shanghai Boer Chemical Reagent Co. Ltd. Ethanol (AR, EtOH) was supplied by Tianjin Fuyu Fine Chemical Co. Ltd. Sodium hydroxide (AR, NaOH), ammonia hydroxide (AR, $NH_3{\cdot}H_2O$) and potassium persulfate (AR, KPS) were purchased from Yantai Shuangshang Chemical Industry Co. Ltd. Distilled water was used in all the experiments.

Preparation of LC-PAVP

First, LC was pretreated with HCl. The dried LC was ground and sieved with a 100 mesh, 10.00 g LC was added to 100 mL HCl solution (4 $mol{\cdot}L^{-1}$) at 80 °C and stirring for 2 h. Then, it was cooled to room temperature. The pretreated LC was filtered and washed with distilled water until the eluant became neutral. The acidifying LC (HLC) was dried at 60 °C for 5 h with 76.5% of yield.

Second, the surface of the loess was modified with KH-570. In a three-necked flask, HLC (5.00 g), H_2O (10 mL) and ethanol (EtOH) (30 mL) were mixed with stirring for 1 h. The pH value adjusted to 3.0–4.0 by acetic acid (HOAc) solution. Adding KH-570 (1.00 g), the mixture was stirred for 30 min at room temperature. Then, the pH value of the mixture was adjusted to 9–10 with ammonia hydroxide ($NH_3{\cdot}H_2O$), heated to 80 °C and stirring for 3 h. The product was filtered and washed with EtOH three times. After vacuum drying at 50 °C for 5 h, silane coupling agent modified loess (KH-LC) (4.87 g) was obtained with 81.20% of yield.

Finally, the LC was modified by surface grafting copolymerization. KH-LC (12.50 g), distilled water (15 mL) and NaOH (0.56 g) was added to a three-necked flask with stirring rod, condenser and nitrogen pipe and stirred. Then, AA (1.45 g) was added drop by drop and stirred mechanically at room temperature for 30 min. NVP (1.1 g) and MBA (0.13 g) were dispersed in distilled water (4 mL) and added into above solution and mechanically stirred for 30 min at 45 °C under nitrogen atmosphere. Then, KPS (0.15 g) was added and the reaction was continued at 80 °C by stirring for 30 min. The obtained product was washed with distilled water three times, and dried at 50 °C, which provided the loess-based grafting copolymer (LC-PAVP) with 96.30% of yield.

Characterization and adsorption properties

LC-PAVP was characterized and analyzed using Fourier-transform infrared spectroscopy (FT-IR), thermal gravimetric analysis (TG), scanning electron microscopy (SEM). Before measuring FT-IR, the samples were ground and sieved with 100–200 mesh. Then, it was mixed with potassium bromide (ratio being 1:100) and compressed to a transparent sheet.

Using LC-PAVP as an adsorbent, the effects of the initial concentration of Pb^{2+}, adsorbent dosage, time, temperatures, pH value, and other factors relating to the adsorption behavior of Pb^{2+} removal were investigated. The adsorption mechanism was discussed using kinetics and adsorption isotherm model. The removal efficiency and adsorption capacity were calculated through Equations (1) and (2):

$$\text{Removal}\% = \frac{C_o - C_e}{C_n} \times 100\% \quad (1)$$

$$\text{Adsorption capacity} = \frac{(C_o - C_e)V}{m} \quad (2)$$

where C_0 is the initial concentration of Pb^{2+} ($mg{\cdot}L^{-1}$) in the solution, C_e is the equilibrium concentration of Pb^{2+} ($mg{\cdot}L^{-1}$) in the solution, V (L) is the volume of the Pb^{2+} solution, and m (g) is the weight of the adsorbent.

RESULTS AND DISCUSSION

Preparation of graft copolymer of acrylic acid onto loess surface (LC-PAVP)

AA and NVP were selected as comonomers because AA is a vinyl monomer with a lower cost and is less polluting to the environment. Due to the carboxyl group (–COOH) in AA, the pH value of its polymers had an effect on the degree of ionization, which further affected the polymerization rate. The homopolymerization of AA is actually the copolymerization of AA and carboxylate (Scott & Peppas 1997), which can be used to prepare microspheres (Yu *et al.* 2014), gels, and so on (Ryu *et al.* 2016). AA can therefore be used for two, three, and multicomponent copolymerization with many monomers (Poggi *et al.* 2015; Yan *et al.* 2015). Acrylic copolymers have been widely used in many fields, such as dyes, water absorbent resins, scale inhibitors, coatings etc. (Cilurzo *et al.* 2010). NVP, a type of lactam compound containing vinyl group, is easily hydrolyzed and polymerized (Parambil *et al.* 2012). The NVP homopolymer and copolymer show good biocompatibility and low toxicity (Reyes *et al.* 2014), which was widely used in food, health care, cosmetics, and other novel materials (Guinaudeau *et al.* 2012; Narayana Reddy *et al.* 2012; Rajeswari *et al.* 2012). A number of copolymers of AA and NVP were prepared (Narayana Reddy *et al.* 2012; Jin *et al.* 2013; Ding *et al.* 2014).

The process for preparation of LC-PAVP is shown in Figure 1. First, the acidifing pretreated loess (LC) was modified by KH-570, which introduced vinyl groups (–CH=CH_2) onto the surface of the loess particles. Then, using AA and NVP as functional comonomers and MBA as a cross-linking agent, loess particles were modified by surface grafting copolymerization, which produced loess-based grafting copolymer (LC-PAVP).

We found that the copolymer could be grafted onto loess particles (KH-LC) using different monomers, and the results are shown in Table 1. However, the yields largely decreased when other monomers (such as 2-hydroxyethyl methacrylate (HEMA) or maleic anhydride (MA)) were used as monomers. It was also found that the ratio of LC:comonomers should be more than 5:1.

The obtained loess-based grafting copolymer (LC-PAVP) was then characterized by SEM, TG, and FT-IR, and compared with intermediates (KH-LC) and materials (LC).

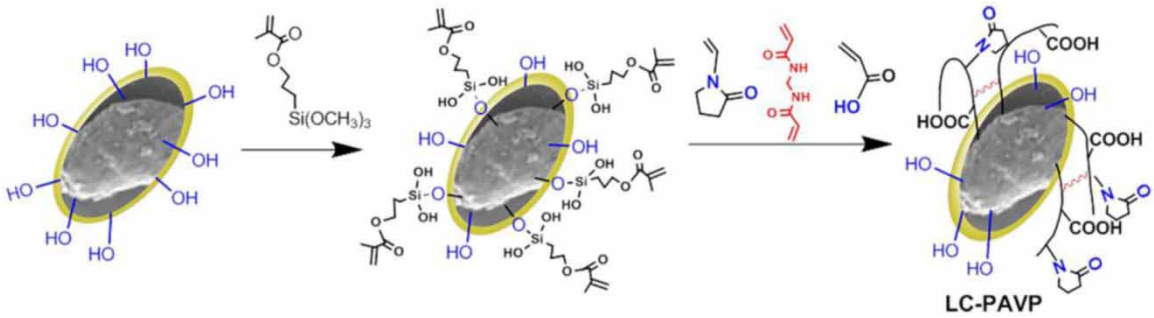

Figure 1 | The process for preparation of LC-PAVP.

Table 1 | The recipes for preparing loess-based grafting copolymer and yields (conditions: grafting copolymerization at 80 °C for 30 min)

Product	KH-LC (g)	NVP (g)	AA (g)	MBA (g)	HEMA (g)	MA (g)	Yield (%)
LC-PAVP(a)	12.5	1.11	1.45	0.13	/	/	96.3
LC-PAVP(b)	4	1.18	0.72	0.09	/	/	78.0
LC-P(VP-HEMA)	4	1.13	/	0.12	1.30	/	82.4
LC-P(VP-MA)	4	1.10	/	0.11	/	1	75.2
LC-P(HEMA-MA)	4	/	/	0.12	1.30	1	56.4

LC/comonomers (g/g): (a) 5/1; (b) 2/1.

SEM images of LC-PAVP

The surface morphology of LC-PAVP was observed by SEM and compared with its materials. The results are shown in Figure 2. It was found that the surface of loess particles (Figure 2(a)) was uneven, porous, very rough and had many small surface cracks. After being modified by KH-570 (Figure 2(b)), some particles were stacked on its surface, and there was not much difference. After modification by grafting copolymers of AA and NVP (Figure 2(c)), the surface of the loess particles became smoother, and a copolymer film was formed on the loess surface that wrapped around the interparticle gaps. The results showed that AA and NVP were grafted by copolymerization onto the surface of loess particles.

FT-IR analysis of LC-PAVP

The FT-IR spectra of LC-PAVP and its materials (LC, KH-LC) are shown in Figure 3. In LC, the absorption peak of the Si–O–Si stretching vibration was near 1,090 cm^{-1}, and the flexural vibration absorption peak of Si–O–Si was near 559 cm^{-1} and 497 cm^{-1}. The characteristic peaks at 3,626 cm^{-1} and 3,450 cm^{-1} can be assigned to the stretching vibration of surface hydroxyl groups (–OH). Flexural

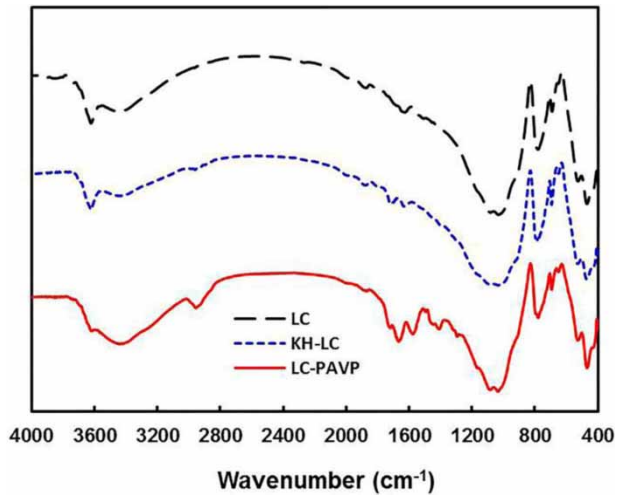

Figure 3 | IR spectra of LC, KH-LC, and LC-PAVP.

vibrations of –OH was near 1,635 cm^{-1} (Tang *et al.* 2009). In KH-LC and LC-PAVP, the main silicate characteristic peaks of the loess (LC) were unchanged. In KH-LC, the characteristic absorption peak of methylene in KH-570 was near 2,950 cm^{-1}. The peak at 1,716 cm^{-1} was the characteristic absorption peak of the ester carbonyl group (Liu *et al.* 2015). In LC-PAVP, the characteristic peaks near 1,716 cm^{-1} and 1,570 cm^{-1} were attributed to symmetric and antisymmetric stretching vibration absorption peak of C=O in COOH (Jin *et al.* 2013; Ma *et al.* 2013), and the peaks around 1,550 cm^{-1} was attributed to N–H in NVP (Roy *et al.* 2013). The bending vibration peak of C–H was near 1,410 cm^{-1} (Rafiee *et al.* 2016). The results showed that AA and NVP were successfully grafted by copolymerization onto the surface of loess.

TG analysis of LC-PAVP

In order to study the thermal stability of LC-PAVP, TG analysis was carried out and compared with LC and KH-LC. The results are shown in Figure 4. In LC, a weight

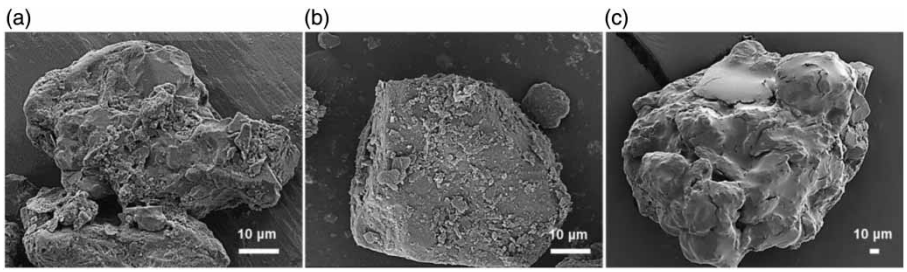

Figure 2 | SEM images of LC (a), KH-LC (b), and LC-PAVP (c).

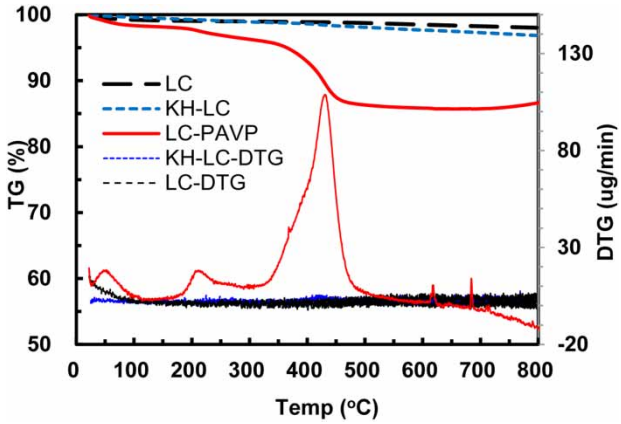

Figure 4 | TG and DTG curves of LC, KH-LC, and LC-PAVP.

loss zone (2%) appeared near 100 °C, which was the water loss of silicate. Water loss was not evident in KH-LC and there was a 3.2% in total weight loss. That meant LC was successfully modified by KH-570. In LC-PAVP, the copolymers of AA and NVP were decomposed between 200 °C and 500 °C, and approximately 10.4% of the weight loss was due to the copolymer chain. Homopolymers of AA and NVP were therefore washed out during preparation, indicating that the copolymer was successfully grafted onto the surface of loess.

Adsorption capacity of LC-PAVP

The obtained LC-PAVP was used to remove Pb^{2+} because it has many hydroxyl groups (–OH) and carboxylates ($–COO^-$). Some reported inorganic adsorbing materials, such as zeolite, kaolinite clay, hydroxyapatite, and pine cone activated carbon, were compared with LC-PAVP. The adsorption capacities of different adsorbent materials for removing Pb^{2+} are shown in Table 2. Compared with other inorganic adsorbing materials, the obtained LC-PAVP is important for the removal of Pb^{2+} from aqueous solution.

Table 2 | The adsorption capacities of different adsorbent materials for removing Pb^{2+}

Adsorbent	The adsorption capacity (mg g^{-1})	References
Hydroxyapatite	41.84	Benhammadi *et al.* (2016)
Pine cone activated carbon	27.53	Milan & Milovan (2011)
Zeolite	14.00	Rakhym *et al.* (2020)
Kaolinite clay	56.18	Unuabonah (2008)
LC-PAVP	68.75	This study

Other parameters related to the effect on the adsorption process, such as initial concentration of Pb^{2+}, adsorbent dosage, time, pH value, and temperature, were also investigated.

Effect of initial Pb^{2+} concentration

The effect of initial Pb^{2+} concentrations was investigated at 25 °C using 0.05 g of LC-PAVP as the adsorbent. Adsorption capacity of LC- PAVP with various initial concentration of Pb^{2+} is shown in Figure 5. If the concentration of Pb^{2+} was lower than 200 mg·L^{-1}, the removal rate was above 98%, and decreased in a small range. The removal rate of LC-PAVP was 98.20% when the concentration of Pb^{2+} was 200 mg·L^{-1}. Subsequently, the removal rate decreased rapidly with the increase in concentration. This may be because the LC-PAVP had enough active sites to bind with Pb^{2+} when Pb^{2+} concentration was low. With increasing Pb^{2+} concentration, the active site of LC-PAVP decreased (Sun *et al.* 2010).

Effect of LC-PAVP dosage

The effect of the amount of adsorbent (LC-PAVP) on the Pb^{2+} adsorption from 50 mL of Pb^{2+} solution (200 mg·L^{-1}) was investigated at 25 °C, and the results are shown in Figure 6. With an increase in the sorbent dosage from 0.01 to 0.08 g, the removal rate of Pb^{2+} also increased noticeably. When LC-PAVP dosage increased from 0.08 to 0.20 g, the removal rate increased slightly. The reason is that all active

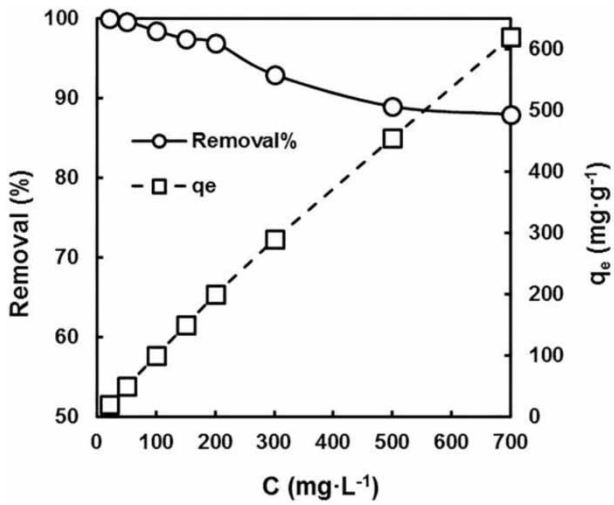

Figure 5 | The effect of initial concentration on the adsorption of Pb^{2+} (conditions: LC-PAVP: 0.05 g; 25 °C).

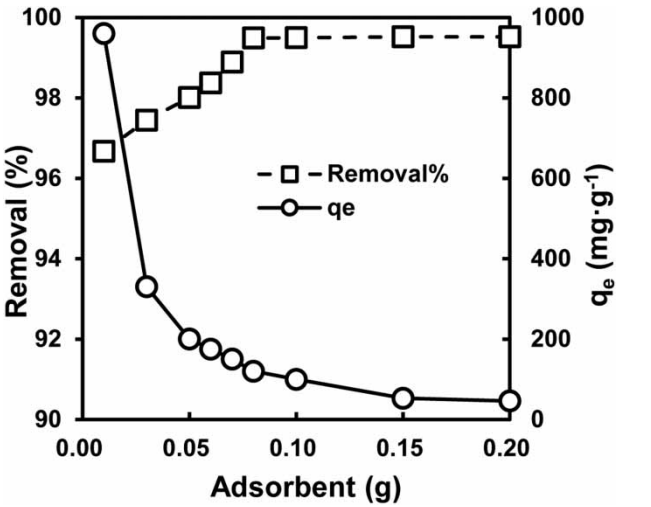

Figure 6 | The effect of adsorbent dosage on the adsorption of Pb^{2+} (conditions: [Pb^{2+}]: 200 mg·L^{-1}; 25 °C).

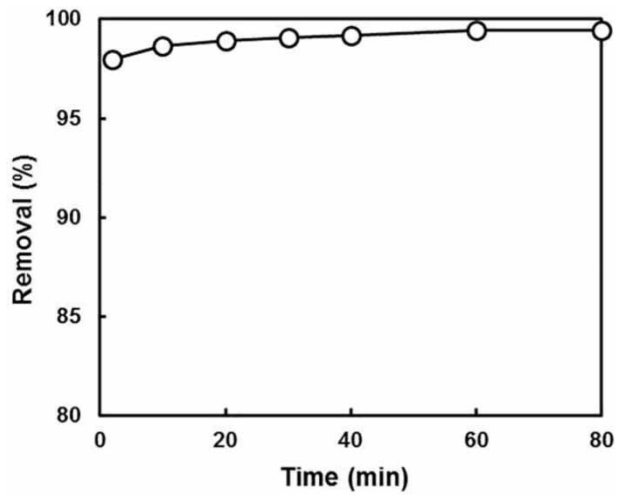

Figure 7 | The effect of contact time on the removal rate of Pb^{2+} (conditions: LC-PAVP: 0.08 g; [Pb^{2+}]: 200 mg·L^{-1}; at 25 °C).

sites on the adsorbent surface are occupied with increasing coverage, the fraction of the bare surface rapidly diminishes, and Pb^{2+} ions have to compete for the adsorption site. An increase in adsorbent dosage will therefore not provide higher uptake of Pb^{2+} (Aroua *et al.* 2008). When the dosage of LC-PAVP increased to 0.08 g, the removal rate of Pb^{2+} reached 99.49%. In relation to cost, the optimal dosage of LC-PAVP was 0.08 g when used in the treatment of Pb^{2+} solutions of 200 mg·L^{-1} concentration.

Effect of time on adsorption

The effect of adsorption time on the removal rate of Pb^{2+} was studied for 50 mL of Pb^{2+} solution (200 mg·L^{-1}) at 25 °C using 0.08 g of LC-PAVP as the adsorbent, and results are shown in Figure 7. Initially, the adsorption rate of Pb^{2+} on LC-PAVP was relatively fast, reaching up to 98.64% within 10 min. The reason was that Pb^{2+} in the solution formed an initial complex with functional groups in the hydroxyl on the surface of LC. Afterwards the adsorption rate increased slowly and gradually. After 60 min, the removal rate reached 99.47% and remained flat. These results may be due to the initiation of LC-PAVP adsorption on Pb^{2+} mainly occurring on the outer surface of the composite, which can be completed in a short time. The repulsive force of Pb^{2+} increased in line with an increase in adsorption capacity. The resistance of free Pb^{2+} to LC-PAVP micropores was also enhanced, and it took longer to reach adsorption saturation (Doğan *et al.* 2009). As a consequence, the optimal adsorption time was 60 min.

Effect of temperature

The influence of temperatures on adsorption of Pb^{2+} solution (200 mg·L^{-1}) was studied using 0.08 g of LC-PAVP as the adsorbent, and the results are shown in Figure 8. The removal rate of Pb^{2+} was above 99.0% at both high and low temperatures, and the highest removal rate of Pb^{2+} was 99.70% at 15 °C. The influence of temperature on the whole adsorption process is not significant. It indicated that the adsorption material was very stable at different temperatures. Adsorption of LC-PAVP on Pb^{2+} can be applied to a wide scope of temperatures.

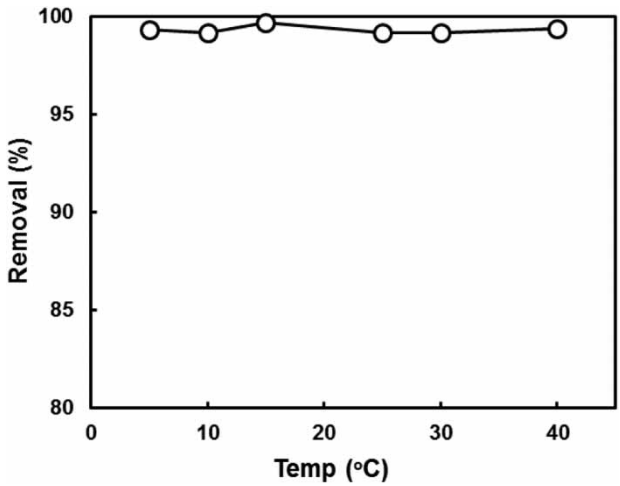

Figure 8 | The effect of temperature on the removal rate of Pb^{2+} (conditions: LC-PAVP: 0.08 g; [Pb^{2+}]: 200 mg·L^{-1}; 60 min).

Effect of pH value

The pH value of the solution was an important factor that may affect adsorbate intake and the degree of ionization that caused the variation in reaction kinetics and equilibrium of the adsorption process (Jin *et al.* 2008). The effect of pH value on the adsorption of Pb^{2+} was measured at 25 °C for 60 min using 0.08 g of LC-PAVP as the adsorbent, and the results are shown in Figure 9. With the increase in pH value from 2.0 to 5.0, the removal rate of Pb^{2+} increased from 95.91% to 99.32%. It was demonstrated that H^+ and Pb^{2+} compete for adsorption sites on the LC-PAVP surface at lower pH values. When the pH value reached 5.44, the removal rate was 99.46%, which was the highest in this experiment. When the pH value was more than 6.0, Pb^{2+} began to form lead hydroxide ($Pb(OH)_2$)), and the precipitates on the surface of LC-PAVP prevented Pb^{2+} from contacting with the active site, which decreased the removal rate (Farooq *et al.* 2010). LC-PAVP can therefore be used in acid environments.

Adsorption kinetics and isotherms

Adsorption isotherms

The isothermal adsorption equation of LC-PAVP for Pb^{2+} can be calculated as per Equations (3) and (4):

$$q_e = \frac{q_m K_L C_e}{1 + K_L C_e} \tag{3}$$

$$q_e = K_f C_e^{\frac{1}{n}} \tag{4}$$

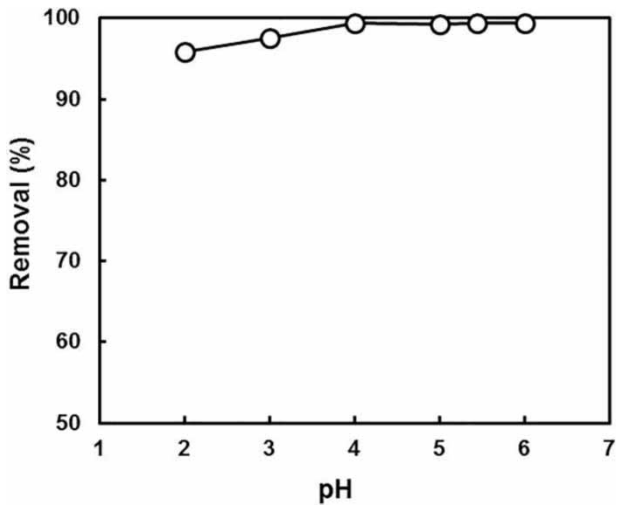

Figure 9 | The effect of pH value on the removal rate of Pb^{2+} (conditions: LC-PAVP: 0.08 g; [Pb^{2+}]: 200 mg·L^{-1}; at 25 °C for 60 min).

where q_e is the adsorbed amount of Pb^{2+} at equilibrium (mg·L^{-1}), q_m is the maximum adsorption capacity (mg·g^{-1}), C_e is the equilibrium Pb^{2+} concentration in solution (mg·L^{-1}), K_L is the Langmuir isotherm constant (L·mg^{-1}), and K_f (L·g^{-1}) and n are Freundlich constants related to the capacity and intensity of adsorption, respectively (Lu *et al.* 2017).

Using Freundlich and Langmuir isothermal models, the nonlinear fitting is made on the relationship between concentration and adsorption capacity. Results are shown in Figure 10 and Table 3. It was closer to the Freundlich equation (Figure 10(b)), and the correlation coefficient got to 0.9858. The maximum adsorption capacity was 68.75 mg·g^{-1}, which fits the Langmuir model in the experiment.

Adsorption kinetics

The experimental data were calculated with adsorption kinetics, and the pseudo-first-order model (Equation (5)) and the pseudo-second-order model (Equation (6)) were applied. Pseudo-first-order model means that the number of sites occupied is directly proportional to the number of sites not occupied; the pseudo-second-order kinetic model assumes the mechanism of chemical reaction, and the adsorption rate is an adsorbent controlled by chemical adsorption through the sharing or exchange of electrons between adsorbate and adsorbent.

$$q_t = q_e(1 - exp^{-k_1 t}) \tag{5}$$

$$q_t = \frac{qe^2 k_2 t}{1 + q_e k_2 t} \tag{6}$$

where q_e is the amounts of Pb^{2+} adsorption (mg·g^{-1}) at equilibrium, q_t is the amounts of Pb^{2+} adsorbed (mg·g^{-1}) at time t (min), k_1 is the adsorption rate constant for the first-order adsorption, and k_2 is the second-order reaction constant.

Nonlinear equations in the measurement of model parameters were more effective than linear equations (Lin & Wang 2009). The results are shown in Figure 11 and Table 4. It was obvious that the pseudo-second-order equation (Figure 11(b)) was better in describing the adsorption kinetics, as shown by the higher determination coefficient ($R^2 = 0.9292$) value, indicating that a chemical reaction is the rate-controlling step (Ho & McKay 1999). The results showed that the chemical adsorption played a primary role in the adsorption of LC-PAVP on Pb^{2+}.

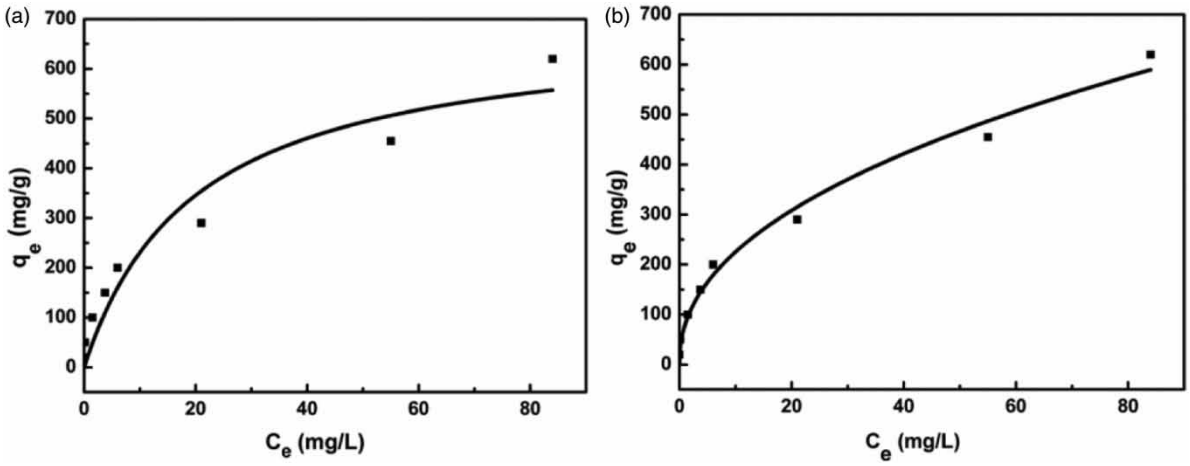

Figure 10 | Isotherms model of Pb^{2+} onto LC-PAVP. Langmuir (a) and Freundlich (b).

Table 3 | Parameters of Langmuir and Freundlich isotherms

Isotherm	Langmuir			Freundlich		
Parameters	q_m (mg·g^{-1})	K_a (L·mg^{-1})	R^2	K_f (mg·g^{-1} (L·mg^{-1})$^{1/n}$)	n	R^2
	68.75	0.0504	0.9277	79.59	2.2126	0.9858

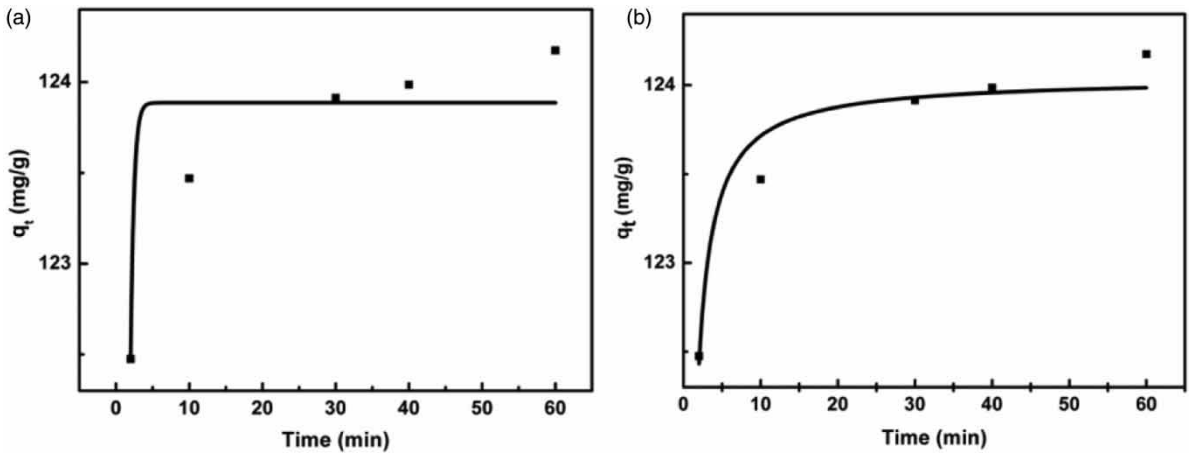

Figure 11 | Kinetics of model of Pb^{2+} onto LC-PAVP. Pseudo-first-order (a) and pseudo-second-order (b).

Table 4 | Kinetic parameters of pseudo-first and second-order adsorption kinetic models

		Pseudo-first-order kinetic			Pseudo-second-order kinetic		
C_0 (mg·L^{-1})	$q_{e(exp.)}$ (mg·g^{-1})	q_{ecal} (mg·g^{-1})	k_1 (min^{-1})	R^2	$q_{e\ cal}$ (mg·g^{-1})	k_2 (g·mg^{-1}·min^{-1})	R^2
200	124.34	123.88	2.2374	0.8084	124.04	0.3070	0.9292

CONCLUSION

To sum up, a novel loess-based polymer absorbent (LC-PAVP) using AA and NVP as functional monomers was successfully synthesized through grafting copolymerization, which significantly reduced the proportion of synthetic polymers. The effects of adsorbent dosage, contact time, system temperature, and initial pH value on the adsorption performance of Pb^{2+} were systematically investigated. The results revealed that LC-PAVP had remarkable capacity of adsorbing Pb^{2+} and had a removal efficiency up to 99.49%. The adsorption process can be explained with the pseudo-second-order type kinetic model and the thermodynamics were best fitted with the Freundlich model. It was concluded that the obtained adsorbent would be a promising, high-efficient and economic material of removing Pb^{2+} in wastewater treatment processes.

ACKNOWLEDGEMENTS

The work was supported by the National Natural Science Foundation of China (Grant No. 21865030, 21364012).

DATA AVAILABILITY STATEMENT

All relevant data are included in the paper or its Supplementary Information.

REFERENCES

Arfin, T. & Tarannum, A. 2019 Rapid determination of lead ions using polyaniline-zirconium (IV) iodate-based ion selective electrode. *Journal of Environmental Chemical Engineering* **7** (1), 102811.

Aroua, M. K., Leong, S. P., Teo, L. Y., Yin, C. & Daud, W. M. 2008 Real-time determination of kinetics of adsorption of lead(II) onto palm shell-based activated carbon using ion selective electrode. *Bioresource Technology* **99** (13), 5786–5792.

Benhammadi, S., Shishkin, A., Iddou, A., Aguedal, H. & De Menorval, L. C. 2016 Adsorption of lead (ii) in liquid-solid interfaces on natural and modified hydroxyapatite. *Key Engineering Materials* **721**, 117–122.

Cilurzo, F., Gennari, C. G., Selmin, F. & Vistoli, G. 2010 Effects of metal ions on entero-soluble poly(methacrylic acid-methyl methacrylate) coating: a combined analysis by ATR-FTIR spectroscopy and computational approaches. *Molecular Pharmaceutics* **7** (2), 421–430.

Ding, Y., Gao, J., Yang, X., He, J., Zhou, Z. & Hu, Y. 2014 Preparation of water dispersible, fluorescent Ag–PAA–PVP hybrid nanogels and their optical properties. *Advanced Powder Technology* **25** (1), 244–249.

Doğan, M., Abak, H. & Alkan, M. 2009 Adsorption of methylene blue onto hazelnut shell: kinetics, mechanism and activation parameters. *Journal of Hazardous Materials* **164** (1), 172–181.

Ecer, Ü., Yılmaz, Ş. & Şahan, T. 2018 Highly efficient Cd (II) adsorption using mercapto-modified bentonite as a novel adsorbent: an experimental design application based on response surface methodology for optimization. *Water Science and Technology* **78** (6), 1348–1360.

Farooq, U., Kozinski, J. A., Khan, M. A. & Athar, M. 2010 Biosorption of heavy metal ions using wheat based biosorbents – a review of the recent literature. *Bioresource Technology* **101** (14), 5043–5053.

Fu, F., Xie, L., Tang, B., Wang, Q. & Jiang, S. 2012 Application of a novel strategy – advanced Fenton-chemical precipitation to the treatment of strong stability chelated heavy metal containing wastewater. *Chemical Engineering Journal* **189**, 283–287. Physics, *227*, 279-290.

Gong, Z., Alef, K., Wilke, B. M. & Li, P. 2007 Activated carbon adsorption of PAHs from vegetable oil used in soil remediation. *Journal of Hazardous Materials* **143**, 372–378.

Guinaudeau, A., Mazières, S., Wilson, D. J. & Destarac, M. 2012 Aqueous RAFT/MADIX polymerisation of N-vinyl pyrrolidone at ambient temperature. *Polymer Chemistry* **3** (1), 81–84.

Hashemzadeh, M., Nilchi, A. & Hassani, A. H. 2019 Synthesis of novel surface-modified hematite nanoparticles for lead ions removal from aqueous solution. *Materials Chemistry and Physics* **227**, 279–290.

He, Y. F., Zhang, L., Wang, R. M., Li, H. R. & Wang, Y. 2012 Loess clay based copolymer for removing Pb (II) ions. *Journal of Hazardous Materials* **227**, 334–340.

Ho, Y. S. & McKay, G. 1999 Pseudo-second order model for sorption processes. *Process Biochem.* **34**, 451–465.

Indah, S., Helard, D. & Sasmita, A. 2016 Utilization of maize husk (*Zea mays* L.) as low-cost adsorbent in removal of iron from aqueous solution. *Water Science and Technology* **73** (12), 2929–2935.

Jin, X., Jiang, M. Q., Shan, X. Q., Pei, Z. G. & Chen, Z. 2008 Adsorption of methylene blue and orange II onto unmodified and surfactant-modified zeolite. *Journal of Colloid and Interface Science* **328** (2), 243–247.

Jin, S., Gu, J., Shi, Y., Shao, K., Yu, X. & Yue, G. 2013 Preparation and electrical sensitive behavior of poly(N-vinylpyrrolidone-co-acrylic acid) hydrogel with flexible chain nature. *European Polymer Journal* **49** (7), 1871–1880.

Kumar, A. S. K., Ramachandran, R., Kalidhasan, S., Rajesh, V. & Rajesh, N. 2012 Potential application of dodecylamine modified sodium montmorillonite as an effective adsorbent for hexavalent chromium. *Chemical Engineering Journal* **211**, 396–405.

Lasheen, M. R., El-Sherif, I. Y., Sabry, D. Y., El-Wakeel, S. T. & El-Shahat, M. F. 2016 Adsorption of heavy metals from aqueous solution by magnetite nanoparticles and magnetite-kaolinite

nanocomposite: equilibrium, isotherm and kinetic study. *Desalination and Water Treatment* **57** (37), 17421–17429.

Li, Y., Liu, S. J., Chen, F. M. & Zuo, J. E. 2019 High-strength apatite/attapulgite/alginate composite hydrogel for effective adsorption of methylene blue from aqueous solution. *Journal of Chemical & Engineering Data* **64** (12), 5469–5477.

Lin, J. & Wang, L. 2009 Comparison between linear and non-linear forms of pseudo-first-order and pseudo-second-order adsorption kinetic models for the removal of methylene blue by activated carbon. *Frontiers of Environmental Science & Engineering in China* **3** (3), 320–324.

Liu, P., Jiang, L., Zhu, L., Guo, J. & Wang, A. 2015 Synthesis of covalently crosslinked attapulgite/poly(acrylic acid-co-acrylamide) nanocomposite hydrogels and their evaluation as adsorbent for heavy metal ions. *Journal of Industrial and Engineering Chemistry* **23**, 188–193.

Liu, X., Bai, X., Dong, L., Liang, J., Jin, Y., Wei, Y. & Qu, J. 2018 Composting enhances the removal of lead ions in aqueous solution by spent mushroom substrate: biosorption and precipitation. *Journal of Cleaner Production* **200**, 1–11.

Lu, T., Wang, L., He, Y., Chen, J. & Wang, R. M. 2017 Loess surface grafted functional copolymer for removing basic fuchsin. *RSC Advances* **7** (30), 18379–18383.

Ma, S., Qi, X., Cao, Y., Yang, S. & Xu, J. 2013 Hydrogen bond detachment in polymer complexes. *Polymer* **54** (20), 5382–5390.

Milan, M. & Milovan, P. 2011 Removal of lead(ii) ions from aqueous solutions by adsorption onto pine cone activated carbon. *Desalination* **276** (1), 53–59.

Narayana Reddy, C. L., Swamy, B. Y., Prasad, C. V., Madhusudhan Rao, K., Prabhakar, M. N., Aswini, C. & Rao, K. C. 2012 Development and characterization of chitosan-poly(vinyl pyrrolidone) blend microspheres for controlled release of metformin hydrochloride. *International Journal of Polymeric Materials* **61** (6), 424–436.

Parambil, A. M., Puttaiahgowda, Y. M. & Shankarappa, P. 2012 Copolymerization of N-vinyl pyrrolidone with methyl methacrylate by Ti (III)-DMG redox initiator. *Turkish Journal of Chemistry* **36** (3), 397–409.

Poggi, E., Guerlain, C., Debuigne, A., Detrembleur, C., Gigmes, D., Hoeppener, S. & Gohy, J. F. 2015 Stimuli-responsive behavior of micelles prepared from a poly (vinyl alcohol)-block-poly (acrylic acid)-block-poly (4-vinylpyridine) triblock terpolymer. *European Polymer Journal* **62**, 418–425.

Rafiee, E., Joshaghani, M. & Abadi, P. G. S. 2016 Effect of a weak magnetic field on the Mizoroki–Heck coupling reaction in the presence of wicker-like palladium-poly(N-vinylpyrrolidone)-iron nanocatalyst. *Journal of Magnetism and Magnetic Materials* **408**, 107–115.

Rajeswari, N., Selvasekarapandian, S., Karthikeyan, S., Nithya, H. & Sanjeeviraja, C. 2012 Lithium ion conducting polymer electrolyte based on *poly (vinyl alcohol) – poly (vinyl pyrrolidone)* blend with $LiClO_4$. *International Journal of Polymeric Materials* **61** (14), 1164–1175.

Rakhym, A. B., Seilkhanova, G. A. & Kurmanbayeva, T. S. 2020 Adsorption of lead (II) ions from water solutions with natural zeolite and chamotte clay. *Materials Today: Proceedings*. https://doi.org/10.1016/j.matpr.2020.05.672.

Reyes, F. T., Guo, L., Hedgepeth, J. W., Zhang, D. & Kelland, M. A. 2014 First investigation of the kinetic hydrate inhibitor performance of poly(N-alkylglycine)s. *Energy & Fuels* **28** (11), 6889–6896.

Roy, S., Yue, C. Y., Venkatraman, S. S. & Ma, L. L. 2013 Fabrication of smart COC chips: advantages of N-vinylpyrrolidone (NVP) monomer over other hydrophilic monomers. *Sensors and Actuators B: Chemical* **178**, 86–95.

Ryu, J., Ko, J., Lee, H., Shin, T. G. & Sohn, D. 2016 Structural response of imogolite–poly(acrylic acid) hydrogel under deformation. *Macromolecules* **49** (5), 1873–1881.

Scott, R. A. & Peppas, N. A. 1997 Kinetic study of acrylic acid solution polymerization. *AIChE Journal* **43** (1), 135–144.

Shen, W., Chen, S., Shi, S., Li, X., Zhang, X., Hu, W. & Wang, H. 2009 Adsorption of Cu (II) and Pb (II) onto diethylenetriamine-bacterial cellulose. *Carbohydrate Polymers* **75** (1), 110–114.

Shen, Y., Wang, Q., Wang, Y., He, Y. F., Song, P. & Wang, R. M. 2019 Itaconic copolymer modified loess for high-efficiently removing copper ions from wastewater. *Journal of Dispersion Science and Technology* **40** (6), 794–801.

Song, J., Oh, H., Kong, H. & Jang, J. 2011 Polyrhodanine modified anodic aluminum oxide membrane for heavy metal ions removal. *Journal of Hazardous Materials* **187** (1–3), 311–317.

Sun, D., Zhang, X., Wu, Y. & Liu, X. 2010 Adsorption of anionic dyes from aqueous solution on fly ash. *Journal of Hazardous Materials* **181** (1–3), 335–342.

Tang, X., Li, Z. & Chen, Y. 2009 Adsorption behavior of Zn (II) on calcinated Chinese loess. *Journal of Hazardous Materials* **161** (2–3), 824–834.

Unuabonah, E. 2008 Removal of lead and cadmium ions from aqueous solution by polyvinyl alcohol-modified kaolinite clay: a novel nano-clay adsorbent. *Adsorption Science and Technology* **26** (6), 383–405.

Wang, Y., Tang, X., Chen, Y., Zhan, L., Li, Z. & Tang, Q. 2009 Adsorption behavior and mechanism of Cd (II) on loess soil from China. *Journal of Hazardous Materials* **172** (1), 30–37.

Yan, J., Huang, Y., Miao, Y. E., Tjiu, W. W. & Liu, T. 2015 Polydopamine-coated electrospun poly(vinyl alcohol)/poly (acrylic acid) membranes as efficient dye adsorbent with good recyclability. *Journal of Hazardous Materials* **283**, 730–739.

Yang, Y., Zhu, R., Chen, Q., Fu, H., He, Q., Zhu, J. & He, H. 2020 A novel multifunctional adsorbent synthesized by modifying acidified organo-montmorillonite with iron hydroxides. *Applied Clay Science* **185**, 105420.

Yu, C. L., Wang, X., Chen, C. & Zhang, F. 2014 Preparation of polystyrene microspheres using rosin–acrylic acid diester as a cross-linking agent. *Industrial & Engineering Chemistry Research* **53** (6), 2244–2250.

Zhang, D., Zhang, C. L. & Zhou, P. 2011 Preparation of porous nano-calcium titanate microspheres and its adsorption behavior for heavy metal ion in water. *Journal of Hazardous Materials* **186** (2–3), 971–977.

First received 2 May 2020; accepted in revised form 20 July 2020. Available online 3 August 2020